The role of endothermic gasification in propellant ignition

Caroline Lowe

Department of Applied Mathematics and Theoretical Physics, Centre of Mathematical Sciences, Cambridge University, Cambridge, England, UK

Received February 2002
Revised May 2003
Accepted May 2003

Keywords *Compressible flow, Ignition systems, Differential equations, Gases*

Abstract *This study explores a reactor model designed to describe the decomposition, ignition and combustion of energetic materials in combination with real experimental data for these energetic materials. Spatial uniformity is initially assumed which reduces the system of partial-differential-equations to a system of ordinary-differential-equations that can be easily solved numerically. The phase-plane is explicitly presented and examined to illustrate how chemistry and temperature evolve in time. The computations provide an understanding of the vast different timescales that exist and illustrate the singularity structure. Following this the effect of including this chemical regime in an environment typically induced by the combustion of these materials, that is within a compressible fluid flow, is pursued.*

Introduction

Energetic materials are the fuel source used in propulsion systems, such as rocket motors, ballistic weapons and explosive devices. During combustion, these materials rapidly release large quantities of chemical energy. The transport and handling of these materials is hazardous and extremely sensitive to local thermal conditions and mechanical shock. This danger has lead to the development of insensitive munitions that are more stable during handling. However, making these materials less volatile in "normal" conditions has also made them harder to ignite reliably during use.

Experiments on these materials have indicated a number of distinct stages in the combustion process. These stages include an initial gasification of the solid, that can be either endothermic or mildly exothermic; what is worth noting is that insensitive munitions display a distinct endothermic gasification process. The gasification produces gaseous reactants that at some point ignite and burn in a very exothermic reaction. A model of a simple chemical system to describe these stages and numerical solutions of single and multi-phase fluids that included this chemistry was presented by Clarke and Lowe (1996) and Lowe and Clarke (1999).

A reactor model for ignition and combustion, presented by Clarke (1996), follows a simple reaction scheme and investigates an endothermic gasification process that provides a supply of gaseous reactive species. The model, as it will be referred herein, assumes that both gasification and gas-phase reactions can be described as Arrhenius-type reactions. This chemical combination

International Journal of Numerical Methods for Heat & Fluid Flow
Vol. 14 No. 4, 2004
pp. 493-511

0961-5539
DOI 10.1108/09615530410532268

illustrates two distinctly different classes of solution depending on the relation between the characteristic times of the chemical reactions. The behaviour of these reduced chemical systems appears to display the attributes of various successful and unsuccessful ignition processes that are known to exist.

If spatial uniformity is assumed then spatial variations can be neglected in the model – a so-called "well-stirred reactor". Consequently, the system is mathematically described by a system of ordinary-differential-equations that describe how the density, reactants and energy change over time. Some simplifications enable the system to be reduced to a single equation that describes the change in one reactant species with temperature. This enables the mathematician to obtain singular points and explore their nature.

Two areas of interest will be pursued in this account: the previous study of the combustion model was able to identify singular points and sketch the nature of the solution. However, the complete solution in the phase plane can only be provided by numerical integration of the system of equations. Further, simplifications assumed in the earlier work – needed to provide an analytically tractable system – will be relaxed with the objective of studying a more "realistic" problem. In this case, the nature of the solution can only be explored by adopting numerics; direct comparisons between the "realistic" and simplified systems will be made.

The second part of the study will focus on non-linear wave interaction with this chemical sequence. The reactor model adopts chemical data obtained from experiments on HMX explosive. The fluid flows created from the combustion of such highly energetic fuels in closed conditions are often of high Mach number. Consequently, the one-dimensional form of the reactive compressible Euler equations are presented and solved using appropriate numerical techniques. The research focuses on how wave motion couples with the chemical behaviour in a closed vessel and the suitability of computational schemes.

The reactor model

A closed container holds inert gas that is hotter than the ambient initial temperature. The hot conditions cause a reactive solid to gasify, creating reactive species P. The requirement of latent heat of vaporisation means that the gasification is an endothermic process. P reacts to produce a further reactant A in a thermally neutral process. Finally, A reacts to provide heat and inert product gas B. The sequence can be summarised:

$$\text{solid fuel} \xrightarrow{\dot{m}} P \xrightarrow{k_1} A \xrightarrow{k_2} B + \text{heat} \tag{1}$$

with reaction rates k_n $(n = 0, 1)$ presumed to be of the form:

$$k_n = \mathscr{A}_n \exp(-E_n/RT). \tag{2}$$

Equation (2) is a typical Arrhenius form with T temperature, E_n activation energy, R gas constant and $\mathscr{A}_n$ is a pre-exponential factor (assumed to be

constant in this study) of dimensions s^{-1}. The gasification is assumed to behave according to a surface pyrolysis in which the rate of gaseous mass addition $\dot{m}$ is a function of surface temperature which is itself a function of gas temperature, such that:

$$v\dot{m} = \mathscr{B} \exp(-E_S/RT) \tag{3}$$

where $v = 1/\rho$ is the specific volume.

The specific total energy E is defined as:

$$E = e + \frac{1}{2}u^2; \quad e = \sum_{i=1}^{N} c_i e_i \tag{4}$$

where u is the gas velocity, c_i is the mass-fraction of each chemical species i, and e_i is the corresponding specific internal energy. Assume that the specific heats at constant volume C_v are constant and the same for all species and the gases are ideal, then the internal energies for the gaseous components are:

$$e_P = e_A = e^{\text{th}} + Q; \qquad e_B = e^{\text{th}}; \quad \text{where } e^{\text{th}} = C_v T; \tag{5}$$

e^{th} is thermal energy per unit mass of each species, T is temperature and Q is the energy of formation. It follows that

$$e = \sum_{i=1}^{N} c_i e_i = e^{\text{th}} + (c_P + c_A)Q$$

and the total energy may then be simplified and given as:

$$E = e^{\text{th}} + (c_P + c_A)Q + \frac{1}{2}u^2. \tag{6}$$

The ideal gas assumption implies that

$$p = \rho RT; \qquad a^2 = \gamma RT = \gamma pv \tag{7}$$

where ρ is density, $v = 1/\rho$ is specific volume, p is pressure, γ is the ratio of specific heats, $R = \mathscr{R}/\mathscr{W}$ is a constant where $\mathscr{R}$ is the universal gas constant, $\mathscr{W}$ is the molecular weight of each gas (which again for simplicity will be assumed to be the same for both oxidant and fuel and by implication for product also) and a is sound-speed.

The equations that govern one-dimensional unsteady behaviour of a compressible gas that reacts according to the scheme given in equation (1) can be put together from information by Clarke and Lowe (1996), as follows:

$$\mathbf{U}_t + \mathbf{F}_x(\mathbf{U}) = \mathbf{S}(\mathbf{U}) \tag{8}$$

where

$$\mathbf{U} = \begin{pmatrix} \rho \\ \rho c_P \\ \rho c_A \\ \rho u \\ \rho E \end{pmatrix}, \qquad \mathbf{F}(\mathbf{U}) = \begin{pmatrix} \rho u \\ \rho u c_P \\ \rho u c_A \\ \rho u^2 + p \\ up(E + pv) \end{pmatrix},$$

$$\mathbf{S}(\mathbf{U}) = \begin{pmatrix} \dot{m} \\ \dot{m} - \rho k_1 c_P \\ \rho k_1 c_P - \rho k_2 c_A \\ \dot{m} u \\ \dot{m}(e_{\text{th}} + pv + k) + \dot{m}(Q - L) \end{pmatrix}.$$

Note that there is no explicit equation necessary for mass fraction c_B, since $c_A + c_P + c_B = 1$.

Summary of ODE form

The spatially uniform equations derived from equation (8) are a system of four ODEs in time. Define quantities $\mathscr{D}_n$ as Damköhler numbers that denote the ratio between the reaction rate and the local flow of gasifying material ($v\dot{m}$):

$$\mathscr{D}_n = k_n / v\dot{m}. \tag{9}$$

In the earlier work, it was assumed that the rate of reaction k_1 is such that $\mathscr{D}_1$ is constant; for this choice of parameter values the equation for c_P can be analytically integrated to give:

$$c_P = (1 + \mathscr{D}_1)^{-1}\{1 - \exp[-(1 + \mathscr{D}_1)]\tau\} \tag{10}$$

where the new independent variable $\tau = \ln[1 + m/\rho_0)]$ and m is the total mass of propellant that has gasified in time t (that is τ is the transformed non-dimensional time).

If it is further assumed that:

$$c_P(0) \equiv (1 + \mathscr{D}_1)^{-1} \tag{11}$$

then c_P will remain constant as long as there is a supply of reactant species. The study by Gray and Scott has examined models of this type (c_P constant – described as "pool-reactant" models), both with mathematics and in the laboratory (Gray and Scott, 1990). It was shown that by making the pool reactant assumption, the model reduced to one single autonomous ODE.

For comparison with earlier study, this single autonomous equation will be presented; define the following non-dimensional system:

$$\theta \equiv \frac{T - T_{\mathrm{a}}}{\sigma T_{\mathrm{a}}}, \qquad \alpha \equiv \frac{c_A}{c_{\mathrm{ref}}} \tag{12}$$

where

$$\tilde{Q} = \frac{Q}{C_v T_{\mathrm{a}}}, \qquad \sigma = \frac{RT_{\mathrm{a}}}{E_2}, \qquad \kappa = \mathscr{D}_2(0), \qquad c_{\mathrm{ref}} = \frac{\sigma}{\kappa \tilde{Q}}$$

and T_{a} is the ambient temperature.

Using these new variables and assumption (equation (11)), the spatially uniform version of system (equation (8)) can be reduced to the following single equation:

$$\frac{\mathrm{d}\alpha}{\mathrm{d}\theta} = \frac{\mu - \kappa\alpha f(\theta) - \alpha}{\alpha f(\theta) - \mathscr{L}_{\mathrm{a}} + (\gamma - 1)\theta} \tag{13}$$

where

$$\nu = E_{\mathrm{S}}/E_2, \qquad f(\theta) = \exp\left[\frac{-(\nu - 1)\theta}{1 + \sigma\theta}\right], \qquad \sigma\mathscr{L}_{\mathrm{a}} \equiv \frac{L}{C_v T_{\mathrm{a}}} - (\gamma - 1),$$

$$\mu \equiv \mathscr{D}_1 c_P / c_{\mathrm{ref}}.$$

This single equation has the capacity to provide two different classes of solution, *providing* the gasification process is indeed endothermic. It should be observed that different regimes provided by the combustion model *only* exist if the combustion process includes an endothermic stage. If no endothermic phase exists then the denominator of equation (13) is always greater than 0; therefore, there will be no singular points of the ODE. Consequently, the combustion model will always eventually result in a successful ignition due to the fact that the exothermic reaction rate k_2 is always non-zero, in this case, the ignition delay will depend on the activation energy E_2. It is only through the introduction of latent heat requirements that failure to ignite and a"slow burn" mechanism (that will be illustrated below) can emerge. This study is not aimed towards characterising how the size of the latent heat effects the combustion; what is of interest are how the opposing endothermic and exothermic reactions and their relative timescales control the ignition and combustion processes. In summary, the role of the endothermic reaction is to enrich the combustion model in terms of providing new mechanisms of ignition and burning that are not available in a model that includes only exothermic behaviour. Therefore, the study assumes constant endothermic latent energy (L(J/kg)) and exothermic combustion energy (Q(J/kg)) but varies the activation energy of these reactions.

The two classes of solution depend on the ratio of the chemical times of the endothermic and exothermic reactions, ν, that is defined in relation to equation (13). Let us reintroduce the initial-value problem defined by Clarke (1996) in which reaction rate data were approximated from the experimental data of Tarver and McGuire on HMX explosive (Table I). Equivalent values of the dimensionless variables are also defined in Table I.

Numerically derived phase planes will be presented using these data for different values of the parameter ν. Two different initial value problems will be pursued.

The first, for comparison and validation purposes, corresponds to the pool reactant model in which c_P remains constant – and non-zero – for all times and $c_A(0) \equiv 0$, that is the solution to equation (13). Recall that earlier studies have sketched the nature of this solution; here the full solution is presented.

The second explores a more realistic problem in which both reactant species $c_P(0) \equiv 0$ and $c_A(0) \equiv 0$. These equations do not reduce to an autonomous form and therefore, the complete solution and all singular points can only be identified numerically. The emphasis will be to clarify whether there is similar behaviour between this solution and the one described in the previous paragraph.

It is easy to show that the system of equations is stiff due to different timescales involved. Consequently, the system of equations was numerically integrated with a semi-implicit algorithm detailed by Press *et al.* (1992).

Case A: $0 \leq \nu \leq 1$

Initial-value-problem $c_P(0) \equiv (1 + \mathscr{D}_1)^{-1}$. For this initial value of c_P the concentration of reactant P remains constant for all time and the system of

T_a	300 K
γ	1.27
$\mathscr{W}$	21 kg/mol
Q	5,000,000 J/kg
$\mathscr{A}_2$	$3.5 \times 10^{19}\,s^{-1}$
$\mathscr{B}$	$1.156 \times 10^{18}\,s^{-1}$
$\mathscr{A}_1 = 9\mathscr{B}$	–
p_0	101,400 Pa
$\mathscr{R}$	8,313 J/kmol
L	416,447 J/kg
E_2	142 kJ
$E_S = \nu E_2$	–
$E_1 = \nu E_2$	–
σ	0.0175
μ	58.47
κ	0.1
$\mathscr{L}_a$	38.78

Table I.
Input parameters

ODEs reduces to equation (13). There is an unstable singularity, namely a saddle-point, in the θ-α plane. For $\nu = 0.9$ this saddle point was predicted to be located at position (0, 53.141). Define locii y_1 and y_2 that follow the nullclines of equation (13) (that is y_1 and y_2 should locate the turning points of the solutions to equation (13) and the intersection of y_1 and y_2 should locate the singular point).

Figure 1 shows the numerical solutions for $T_0 = 395,\ 396,\ 400\,\mathrm{K}$ and $c_A(0) \equiv 0$. Define the critical initial dimensionless temperature as θ_{crit} that separates a successful ignition from an unsuccessful ignition. This is located at the dimensional temperature $T_{\mathrm{crit}} \approx 395\,\mathrm{K}$: when $\theta_0 = \theta_{\mathrm{crit}} - \Delta\theta$, where $\Delta\theta$ is some small change in θ, the temperature continues to decrease as the reactant mass-fraction increases – this corresponds to the physical situation in which latent heat requirements are always greater than the exothermic activity in the gas-phase and ignition of the gas-phase fails. Over time, the temperature will continue to decrease and the reactant mass increases.

For $\theta_0 = \theta_{\mathrm{crit}} + \Delta\theta$, the temperature initially decreases, again due to latent heat requirements. However, as the reactant gases accumulate in the chamber, eventually sufficient exothermic activity arises for the reactant mass to decrease, due to consumption of the reactant, temperature starts to increase and eventually thermal runaway (ignition) is established. In this study, the time taken between time zero and thermal runaway will be described as the induction time t_{ind}.

Equivalent behaviour has been seen before for a simpler chemical scheme, as detailed by Clarke and Lowe (1996). Consider the timescales associated with these solutions; for $T_0 \equiv 400\,\mathrm{K}$, the history of the temperature and mass-fraction c_A is shown in Figure 2(b). For this initial temperature, the

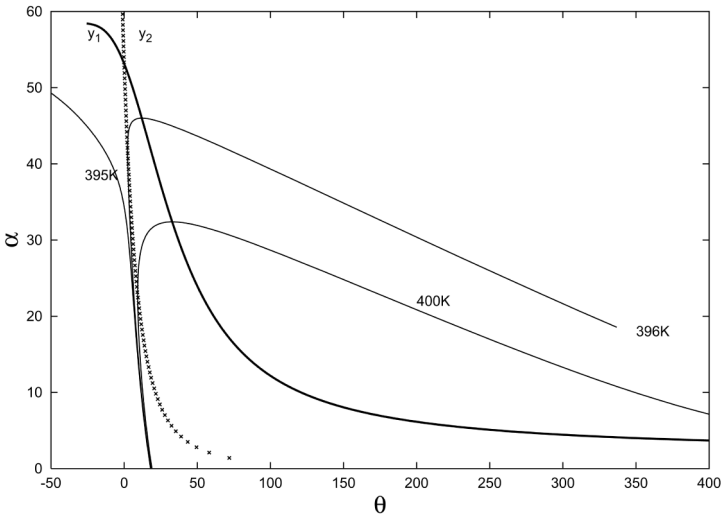

Figure 1.
Phase plane for the reactor model with $\nu = 0.9$ and $c_P(0) \equiv (1 + \mathscr{D}_1)^{-1}$

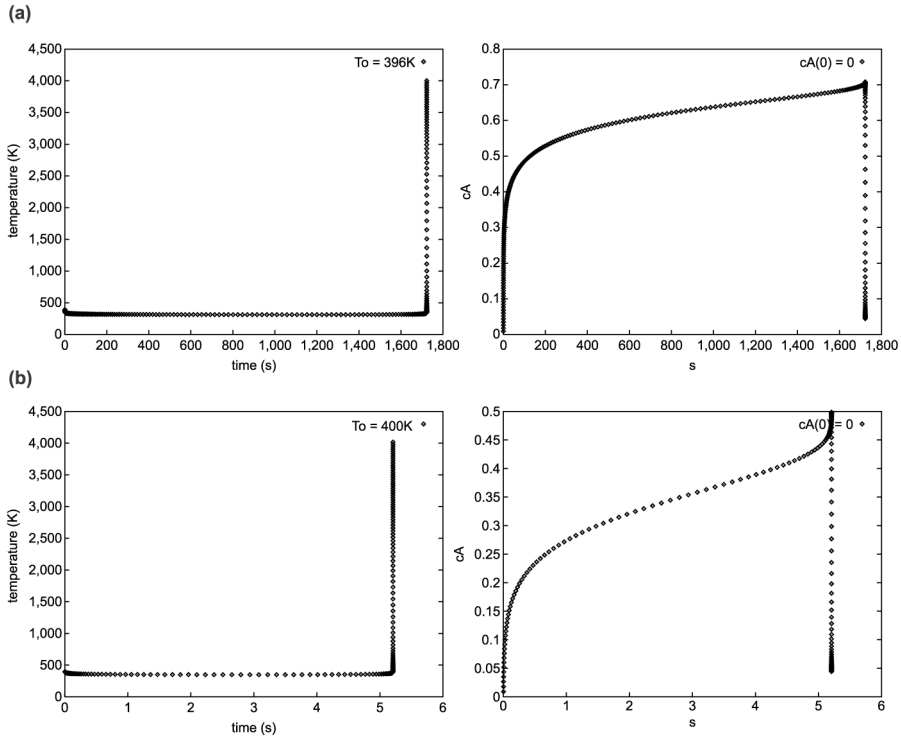

Figure 2.
Temperature and mass-fraction c_A histories for the reactor model with $\nu = 0.9$ and $c_P(0) \equiv (1 + \mathscr{D}_1)^{-1}$. Initial conditions
(a) $T_0 = 396\,\mathrm{K}$,
(b) $T_0 = 400\,\mathrm{K}$

time to ignition is $t_{\mathrm{ind}} \approx 6\,\mathrm{s}$; this is much longer than would be desirable in an actual propulsion system for example, in a ballistic device the complete combustion event (i.e. from ignition to material completely burning out) should last for about 10 ms. As the trajectories in the phase plane approach the singular point time increases by several orders of magnitude, as shown in Figure 2(a) for $T_0 = 396\,\mathrm{K}$. It was speculated that trajectories close to the saddle point describe a "hang-fire" situation in which ignition occurs, but only after an unacceptably long delay.

Initial-value-problem $c_P(0) \equiv 0.0$. In this case, the variation in c_P over time means that the type of analysis seen above, in which the system of equations can be reduced to one single equation, is no longer possible. Figure 3 shows three-dimensional numerical solutions for $T_0 = 400$ and 420 K and $c_A(0) = 0$ with corresponding θ-α plane. It can be seen that the behaviour is broadly similar to that shown in Figure 1, only the critical temperature has increased, for the case in which $T_0 = 400\,\mathrm{K}$ there is no successful ignition. The similarity of the solution is not surprising on examination of the corresponding c_P history for $T_0 = 420\,\mathrm{K}$ (Figure 4); c_P rapidly attains the final value 0.1 and other than this, initial short transient behaves as a pool-reactant.

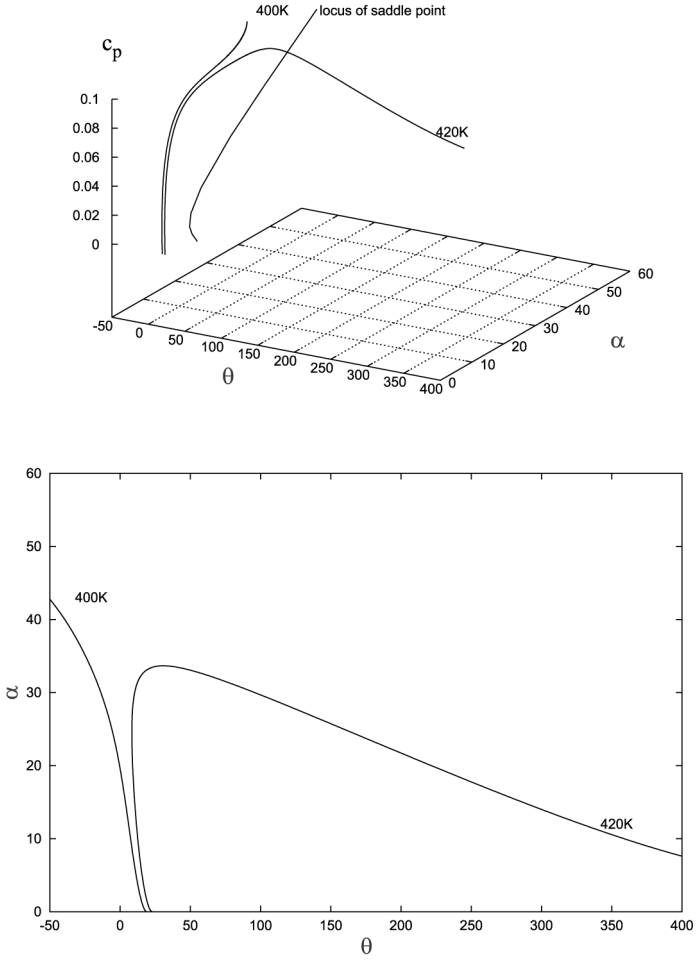

Figure 3.
Phase plane for the reactor model with $\nu = 0.9$ and $c_P(0) = 0$

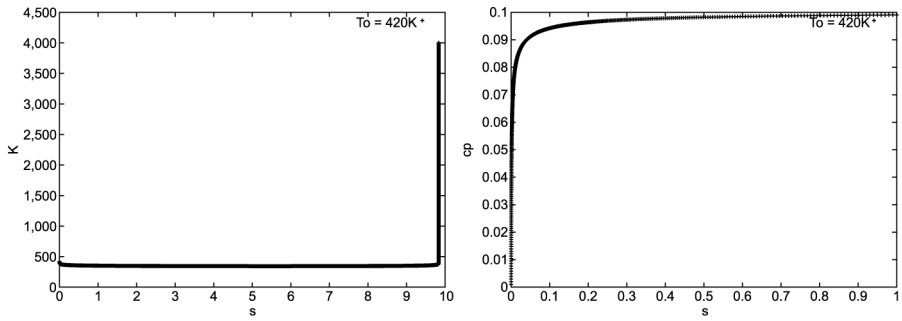

Figure 4.
T and c_P for the reactor model with $\nu = 0.9$, $c_P(0) = 0$ and initial conditions $T_0 = 420\,\mathrm{K}$

It is seen that for the choice of parameters made in this study, the relaxed more general system behaves in a similar manner to the reduced system in the section previous. The rate of increase of c_P relies on the rate of change of dimensionless variable τ (equation (10)) which depends on $\dot{m}$. If the parameter values were such that the rate of increase of c_P were much slower, then μ would increase slowly with c_P thus perturbing the ODE (equation (13)) over longer times. The saddle point is no longer fixed in (θ, α) space but varies with c_P (Figure 3). Figure 4 shows that for $T_0 = 420\,\mathrm{K}$, the ignition time is $\approx 10\,\mathrm{s}$; for the case in which c_p is constant throughout, the ignition time is only 0.03 s – almost three-orders of magnitude smaller. Although the qualitative behaviour of the complete and reduced systems of ODEs is similar, the quantitative behaviour differs enormously.

Case B: $1 < \nu$

Initial-value-problem $c_P(0) \equiv (1 + \mathscr{D}_1)^{-1}$. For the pool-reactant model, there are two singular points for these values of ν. The first is, as above, located at position (0, 53.141), but corresponds to a stable node. The second singularity is located at (194.21, 58.39) and is an unstable saddle point.

Figure 5 shows the phase-plane including trajectories corresponding to initial conditions $T_0 = 1,328\,\mathrm{K}, 1,329\,\mathrm{K}, c_A(0) = 0$ along with curves y_1 and y_2. Note that the curve y_2 is a continuous curve that leaves the picture at position (3, 70), attains a maximum and then re-enters the picture at (195, 70). In this case, the critical temperature θ_{crit} is much higher; corresponding to a temperature of approximately 1,328 K.

If the initial temperature is such that $\theta = \theta_{\mathrm{crit}} + \Delta\theta$, then thermal runaway will eventually occur. However, if $\theta = \theta_{\mathrm{crit}} - \Delta\theta$, then the temperature decreases and the reactant mass-fraction grows. As before, the system fails to

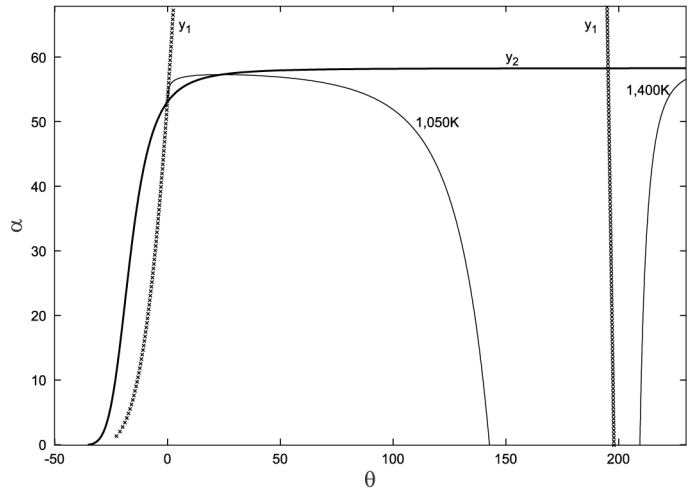

Figure 5.
Phase plane for the reactor model with $\nu = 1.1$ and $c_P(0) \equiv (1 + \mathscr{D}_1)^{-1}$

ignite but in this case, all integral curves will approach a minimum temperature, namely 300 K, and maximum mass-fraction $c_A = 0.9$ at the node (note that the remaining gas will be composed of the pool reactant $c_P = 0.1$). Let us focus on the additional feature which is the history of trajectories in the phase plane that approach the stable node. Figure 6 shows the timescales for this process that are composed of two distinct stages. The first stage consists of an extremely rapid reduction in temperature from 1,328 K to approximately 420 K in approximately 1 s followed by a slow decline to 330 K that takes more than a day! Again, it was suggested that this would adequately represent a "misfire" situation in which thermal runaway does not occur but nevertheless, the material is gasifying and "cooking" over a prolonged time until the point at which the supply of solid material has been completely gasified. The mass-fraction c_A rapidly increases to 0.9 and then starts to decline slowly; for this problem, the reactor system gas is composed of mostly c_A and pool reactant $c_P = 0.1$ indicating that the secondary exothermic reaction is occurring very slowly.

Initial-value-problem $c_P(0) \equiv 0$. Figure 7 shows the equivalent simulation that now sets c_p to zero initially – included are the locii of node and saddle points. In this case, there is negligible difference between the ignition time associated with the initial condition $T_0 = 1,400\,\mathrm{K}$ whether $c_P(0) \equiv 0$ or $c_P(0) \equiv (1 + \mathscr{D}_1)^{-1}$. Similarly, the times associated with the path towards the stable node for the case in which $T_0 = 1{,}050\,\mathrm{K}$ remain virtually the same. On examination, the close similarity – both qualitative and quantitative – between the phase planes in (θ, α) space for the complete and reduced systems is associated with a very rapid increase of c_P to the pool-reactant value.

The one-dimensional problem

It is of interest to identify under what fluid flow regime it may be possible to induce ignition for the reactor model explored earlier. Compressible flows involve shocks, expansion waves and contacts; a test problem that involves all of these features is a standard shock tube problem. The inert shock tube problem is given by equation (8) in which all the terms on the right-hand side

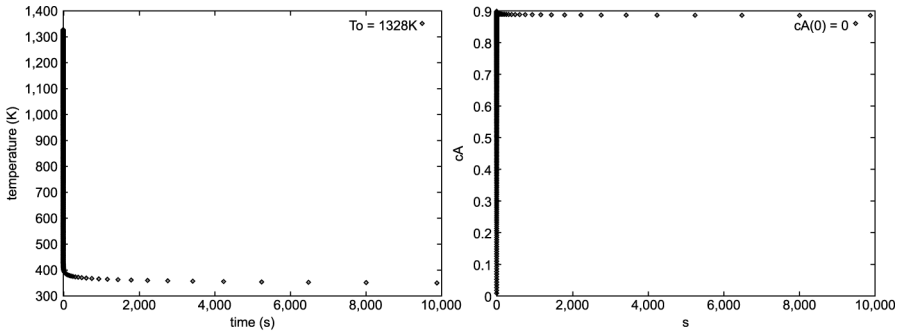

Figure 6.
Temperature and mass-fraction c_A histories approaching the stable-node. Initial conditions $T_0 = 1{,}328\,\mathrm{K}$ and $c_P(0) \equiv (1 + \mathscr{D}_1)^{-1}$

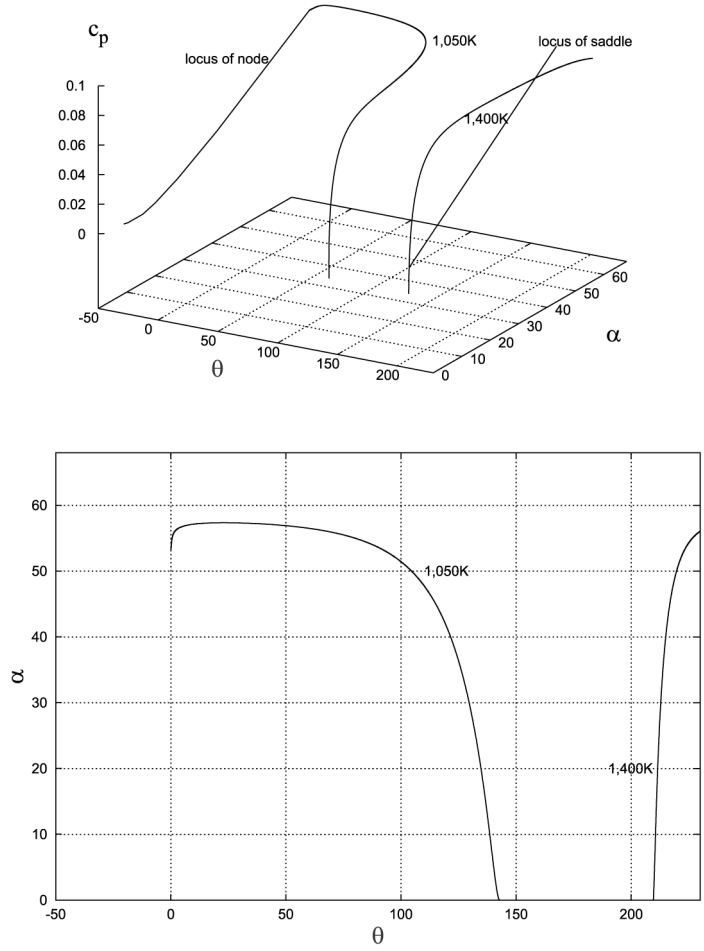

Figure 7.
Phase plane for the reactor model with $\nu = 1.1$ and $c_P(0) \equiv 0$

(source terms) are set to zero. The reactive system of equations is given by equation (8) including the source terms.

The standard technique of time-operator splitting will be employed to solve equation (8). This involves splitting this non-homogeneous hyperbolic problem into two sub-problems, a system of ordinary-differential-equations and a homogeneous hyperbolic system. The former can be solved as above and the latter using shock-capturing methods (Lowe, 1996).

Test problem for $\nu = 0.9$

Initially, explore the case in which $\nu = 0.9$. Consider a domain of length 1 m with initial conditions:

$$T(x,0) = 355\,\mathrm{K}, \qquad c_A(x,0) = 0, \qquad c_P(x,0) = 0,$$
$$p = \begin{cases} 101,400, & x \le 0.5\,\mathrm{m}; \\ 5 \times 101,400, & x > 0.5\,\mathrm{m}. \end{cases} \tag{14}$$

For reference purposes, Figure 8 shows two solution profiles for the inert shock tube problem with a mesh of 1,000 cells. The graphs include the density and temperature at 0.7 and 0.95 ms. At $t = 0.7$ ms, the standard solution consists of an expansion wave that is travelling to the left with head at location $x \approx 0.2$ m and tail at $x \approx 0.43$ m at this time. Similarly, a shock wave is travelling to the right and is at position $x \approx 0.92$ m and a contact discontinuity is at $x \approx 0.69$ m. The temperature ahead of the contact discontinuity and behind the shock, location $0.69 < x < 0.92$, is approximately 421 K. Consequently, it might be expected that the reactive system would result in a successful ignition since this is above the critical ignition temperature. The domain is closed, which means that when the shock wave meets the right boundary at about 0.84 ms it reflects; the solution at time $t = 0.95$ ms illustrates how the temperature behind the reflected shock jumps to $T \approx 493$ K.

Figure 9 shows the flow variables for the reactive case at 0.7 and 0.847 ms. Included are the additional variables that describe the chemical progress c_P, c_A and Damköhler number $\mathscr{D}_2$. The growth in mass-fraction c_P indicates that gasification has been initiated due to the elevated temperature between the contact and shock, $0.69 < x < 0.92$. The profile for c_A indicates that some of this reactant has been converted from c_P to c_A within this region. The endothermic gasification process required to create c_P has a direct effect on the temperature in this region – it is no longer constant as in the inert case – due to latent heat requirements. The temperature does not experience runaway at this time; the reason for this is the induction time associated with this initial temperature (Figure 4). It takes approximately 10 s for the reactor with initial conditions $T_0 = 421$ K, $c_P(x,0) = 0$, $c_A(x,0) = 0$ to ignite under uniform conditions. Some exothermic activity is occurring as seen from the increase in $\mathscr{D}_2$ from zero. If the chamber was not closed, then the wave motion would be sustained and it would take about 10 s for ignition to occur.

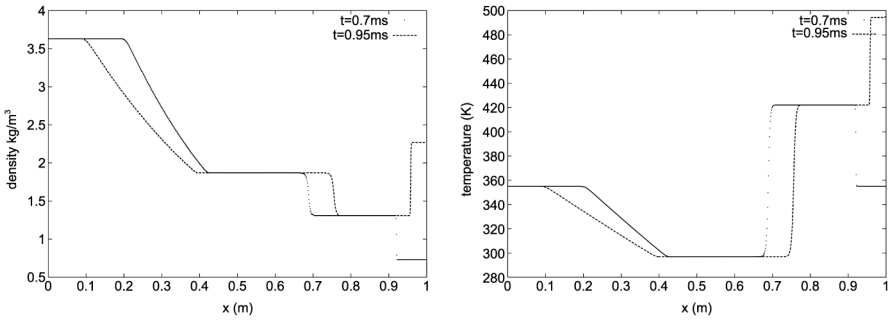

Figure 8.
Profiles at $t = 0.7$ and 0.95 ms for the inert shock-tube problem $T_0 = 355$ K

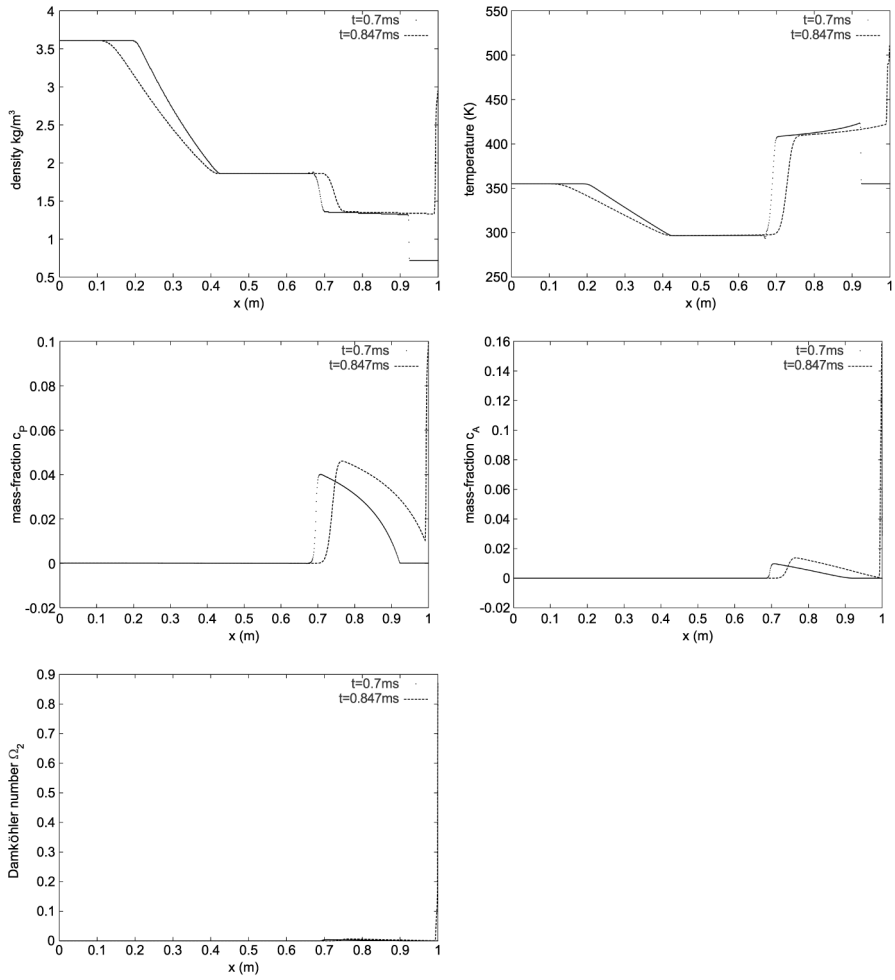

Figure 9.
Profiles at $t = 0.7$ and 0.847 ms for the reactor model with $\nu = 0.9$, $T_0 = 355\,\mathrm{K}$

Consider the later events at 0.847 ms. c_P is only non-zero ahead of the contact that has moved from 0.69 to 0.72 m. The reason for this is two-fold; reactant c_P that existed between $0.69 < x < 0.72$ at time $t = 0.7$ ms has been carried by the local velocity ahead of the contact. Further c_P can no longer be locally created between $0.69 < x < 0.72$ m as at 0.847 ms, the temperature here is 300 K – at this temperature, negligible gasification occurs. Ahead of the contact and behind the shock, c_P continues to increase due to the combined effect of convected c_P along with local production due to the high temperatures immediately ahead of the contact. There is no c_P ahead of the shock wave as the local temperatures are too low and convected material is travelling slower than the shock wave. Since the shock reflects from the right-hand boundary, the

temperature at the boundary experiences a step increase to $T \approx 490\,\mathrm{K}$. The increased temperature at this boundary will change the course of events: referring back to the phase plane for some insight of chemical timescales at these temperatures; for initial conditions $T_0 = 490\,\mathrm{K}$, $c_P(x,0) = 0$, $c_A(x,0) = 0$, numerical simulations have indicated that the induction time is approximately 0.06 ms and it will also take approximately the same time for the mass-fraction c_P to attain its maximum, $c_P = 0.1$. These events are translated to the history of events at the right-hand boundary (Figure 10). After the shock has reflected, c_P starts to rapidly increase whilst the temperature starts to decrease first due to latent heat requirements. It actually takes much less than 0.06 ms after the reflection, for ignition to be induced since the reflected shock is interacting with convected mass-fractions c_P and c_A still travelling towards the right-hand boundary (as these lag behind the shock). After this time, the timescale of the chemical reaction is much smaller than that associated with convection; the characteristic time of the chemical reaction is approximately $t_{\mathrm{reac}} = O(10^{-11})$ whilst the wave motion timestep associated with the Courant condition is $t_{\mathrm{conv}} = O(10^{-6})$. Computing much further after this point would not only take many computational hours but also it is likely that discontinuous waves would not be captured correctly – the difficulty associated with numerical solutions for these types of problems will be explored further in the next section. Any practical computation would benefit from assuming that the

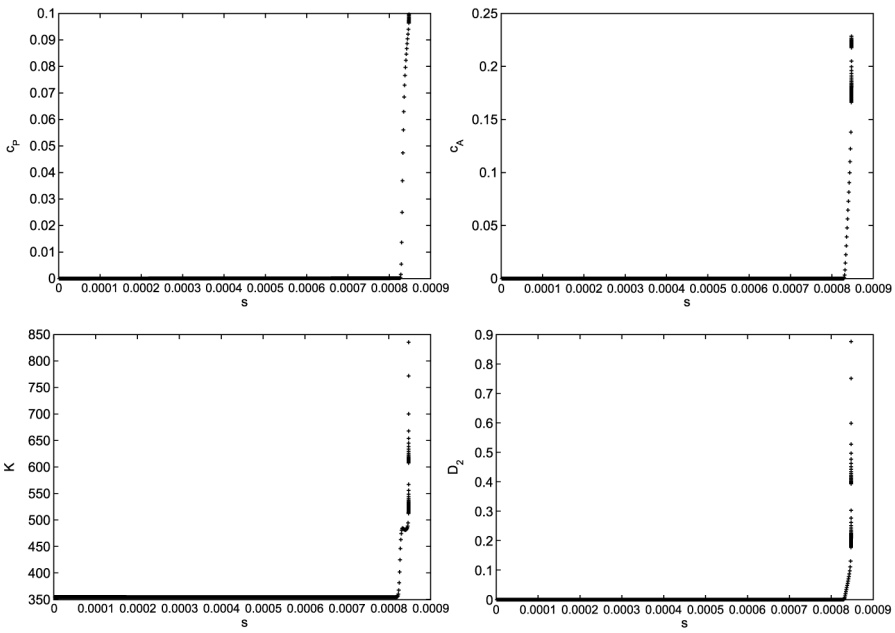

Figure 10.
History at right-hand boundary for $\nu = 0.9$ and $T_0 = 355\,\mathrm{K}$

chemistry is occurring so fast that equilibrium conditions could be assumed, as examined by Clarke and Lowe (1996) and Lowe and Clarke (1999).

The case above involved conditions such that one shock reflection was sufficient to provoke ignition. Generally, the location of the saddle point (Figure 3) controls the go/no-go criteria and how many shock reflections (from the sides of the chamber) are necessary before ignition will occur will depend on this saddle point. *If* the system is completely adiabatic (as assumed) there is an infinite supply of solid reactant, eventually the gas must ignite. However, this would not necessarily be the case if additional physics, such as heat-loss from the reactor, were included in the calculation.

Test problem for $\nu = 1.1$

Initial conditions for the shock-tube problem will be given as:

$$T(x,0) = 1,050\,\mathrm{K}, \qquad c_A(x,0) = 0, \qquad c_P(x,0) = 0,$$

$$p = \begin{cases} 101,400, & x \leq 0.5\,\mathrm{m}; \\ 1,014,000, & x > 0.5\,\mathrm{m}. \end{cases} \tag{15}$$

As above, we wish to explore the case in which local flow conditions provide temperatures above the critical temperature; to achieve this the initial temperature of the shock-tube problem is higher and so is the initial pressure ratio compared to the earlier section. In the case $\nu = 1.1$, recall that the critical temperature for ignition is $T_{\mathrm{crit}} \approx 1,328\,\mathrm{K}$. In Figure 11, the inert solution indicates that the local temperature ahead of the contact is above T_{crit} and one might therefore expect a successful ignition at some point during the wave propagation.

Figure 12(a) and (b) shows the temperature and mass-fraction c_A for the reactive problem at 0.05 and 0.1 ms, respectively. At 0.05 ms, it is clear that the temperature has radically fallen to about half the initial temperature throughout most of the domain. This occurs due to the rapid timescales associated with the chemical rates for initial conditions $T_0 = 1,050\,\mathrm{K}$ – this is

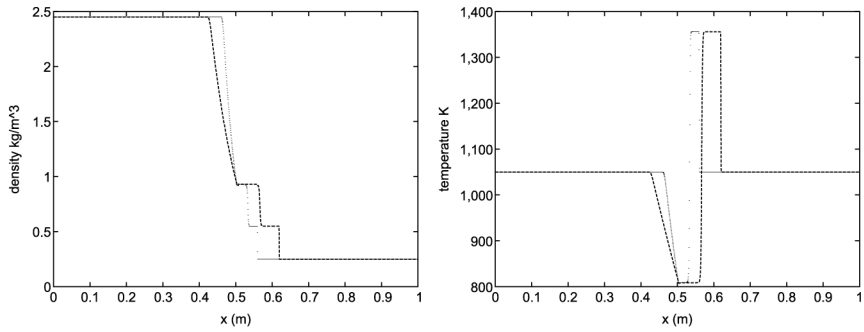

Figure 11.
Profiles at $t = 0.05$ and 0.1 ms for the inert shock-tube problem $T_0 = 1{,}050\,\mathrm{K}$

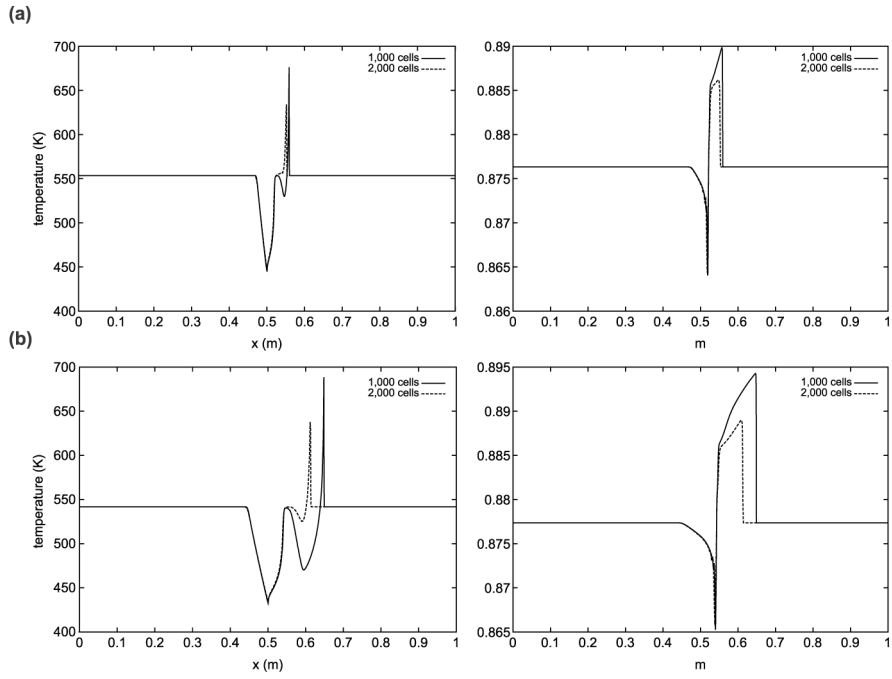

Figure 12. Temperature and mass-fraction c_A profiles at (a) 0.05 ms and (b) 0.1 ms for the reactor model with $\nu = 1.1$, $T_0 = 1{,}050$ K

similar to the behaviour shown in Figure 6 in which the temperature reduces by half in less than 1 μs. At this time, mass-fraction c_P has already arrived at the theoretical maximum $c_P = 0.1$ and it can be seen from the plot c_A (Figure 12(a)) that most of the remaining gas in the chamber is composed of reactant mass-fraction c_A – at these low temperatures negligible amounts of c_A are reacting to give product gas.

After this dramatic behaviour the solution follows a much slower progress towards the stable node but perturbed by wave motion. In this situation, reactant gasification is continuing but at temperatures which are too low and therefore prevent gas-phase thermal runaway from occurring.

However, in this case there were problems with gaining convergence in the solution of the propagating shock. Figure 12(a) and (b) compares solution for a 1,000 cell mesh and 2,000 cell mesh; the fine mesh solutions indicate a different shock wave location – this is particularly visible at time $t > 0.05$ ms.

Numerical experiments indicate that the shock position depends on both space and time discretisations. This type of phenomenon is well documented in the literature for problems that involve non-equilibrium chemistry. More generally, hyperbolic systems that include stiff source terms (that is the timescales associated with the source terms are much shorter than those associated with the homogeneous hyperbolic system) are difficult to solve numerically. As discussed by LeVeque and Yee (1990), the non-physical

propagation of discontinuous features is *not* associated with either the use of an explicit shock-capturing methods or time-operator splitting – the chosen method of solution adopted here. Leveque compared an implicit predictor-corrector method, that did not require any splitting, with an explicit split method – both provided non-physical grid dependent shock-speeds. In fact, the reason for the problem is associated with the intrinsic numerical diffusion that is an attribute of *all* shock-capturing methods. Solution points that fall within the numerical "discontinuity" (due to numerical diffusion) will be rapidly taken to some (non-physical) equilibrium value due to the source terms. The effect of this is a shock moving at a grid-dependent speed since the number and position of points within the numerical discontinuity depend on the mesh size.

A shock-tracking method that explicitly tracks discontinuous features is a possible solution to this problem however, the extension of these methods to general multidimensional systems is still unproven. This study suggests that since the timescales associated with the chemistry are so much faster than the times associated with acoustic wave propagation it may be possible to derive a quasi-steady theory or ignition sub-model to make the application of this model practical.

Conclusions

The reactor model has been analysed for two different types of initial value problem. The first in the spatially uniform regime in which the singular points have been numerically located and the system integrated to provide the complete phase plane. The phase plane diagrams differ depending on the ratio of the activation energies of the endothermic gasification and the exothermic gas-phase combustion. The more realistic problem that cannot be analytically examined, that is the case in which there is initially neither reactant species P nor A in the vessel, has also been pursued and compared with earlier analytical studies. The effect of this additional degree of freedom does not qualitatively change the nature of the solution for the parameter set adopted, but the actual size of the timescales can change significantly. The model displays a number of different initiation events that could represent both successful and unsuccessful ignition processes that is known to occur.

The second type of initial value problem has involved the solution to the Euler equations including the source terms defined by the reactor model. Consequently, the solution combines chemical timescales associated with the rapidly changing source terms in combination with normal compressible flow dynamics. The work involved developing numerical solutions of what is a difficult problem due to the vastly different timescales involved – an understanding of the simple phase plane has been very valuable in this process. The role of singularities and different timescales that exist in the phase plane

(associated with the chemistry alone) has been translated to a more complex problem that involves coupling with the local flow conditions.

Future work must resolve the difficulties associated with these different timescales. The study suggests that numerical methods that explicitly track interfaces might prevent the difficulties associated with mesh convergence however, the radically different scales between the chemistry and the flow imply that asymptotic techniques might be a better solution methodology for this parameter set that involves chemical reactions of high activation energy. Clearly, if this is relaxed and the activation energies were reduced then the numerical solution described above would be the preferred choice as this methodology is easily extendible to more general multidimensional systems.

In this particular study, assumptions associated with the Damköhler number $\mathscr{D}_1$ were made to help make direct comparisons with the earlier theoretical study – this could be relaxed in further work. The effect of heat-loss on the reactor model would be interesting to deduce whether a greater range of solution is possible.

This study does not take explicit account of volume-fraction associated with the gasification of solid material, that is two-phase effects. A more sophisticated model for the solid gasification might include the computation of the solid-surface temperature T_s. This would mean that the gasification rate would be an Arrhenius expression based on T_s, rather than inferring that an Arrhenius rate based on gas temperature is sufficient.

References

Clarke, J.F. (1996), "A reactor model for ignition and burning of a gasifying solid", *Journal of the Chemical Society: Faraday Transactions*, Vol. 92 No. 16, pp. 2951-8.

Clarke, J.F. and Lowe, C.A. (1996), "Combustion with source flows", *Mathematical and Computer Modelling*, Vol. 24 No. 8, pp. 95-104.

Gray, P. and Scott, S.K. (1990), *Chemical Oscillations and Instabilities: Non-linear Chemical Kinetics*, Clarendon Press, Oxford.

Lowe, C.A. (1996), *CFD Modelling of Solid Propellant Ignition*, PhD thesis, Cranfield University Press, Cranfield, Bedfordshire.

Lowe, C.A. and Clarke, J.F. (1999), "Aspects of solid propellant combustion", *Philosophical Transactions of the Royal Society*, Vol. 357 No. 1764, pp. 3639-54.

Press, W.H., Teukolsky, S.A. and Vetterling, W.T. (1992), *Numerical Recipes in Fortran: The Art of Scientific Computing*, 2nd ed., Cambridge University Press, Cambridge.

LeVeque, R.J. and Yee, H.C. (1990), "A study of numerical methods for hyperbolic conservation laws with stiff source terms", *Journal of Computational Physics*, Vol. 86, pp. 187-210.

Further reading

Lowe, C.A. and Clarke, J.F. (2001), "The Euler equations with source terms revisited", *Godunov Methods: Theory and Applications*, Kluwer Academic/Plenum, Dordrecht/New York, NY.